

# SteerTrack: Acoustic-based Device-free Steering Tracking Leveraging Smartphones

Xiangyu Xu\*, Jiadi Yu\*<sup>†</sup>, Yingying Chen<sup>†</sup>, Yanmin Zhu\*, Minglu Li\*

\*Department of Computer Science and Engineering, Shanghai Jiao Tong University, Shanghai, P.R.China

Email: {chillex,,jiadiyu,yzhu,mlli}@sjtu.edu.cn

<sup>†</sup>Department of Electrical and Computer Engineering, Rutgers University, New Jersey, USA

Email: yingche@scarletmail.rutgers.edu

<sup>‡</sup>Corresponding Author

**Abstract**—Given the increasing popularity, mobile devices are exploited to enhance active driving safety nowadays. Among all safety services provided for vehicles, tracking the rotation angle of steering wheel in real time can monitor the vehicles' dynamics and drivers' behaviors at the same time. In this paper, we propose a steering tracking system, *SteerTrack*, which tracks the rotation angle of steering wheel in real time leveraging audio devices on smartphones. *SteerTrack* seeks a device-free approach for steering tracking without requiring installation of specialized sensors on steering wheels nor asking drivers to wear sensors on their wrists. Since the steering wheel is operated by a driver's hands, the rotation angle of steering wheel can be tracked based on movements of the driver's hands. *SteerTrack* first builds an acoustic signal field inside of a vehicle and then analyzes the echoes reflected from the driver's hands with *relative correlation coefficient (RCC)* and *reference frame* to track the movement trajectory of hands under different steering maneuvers. Given the tracked movement trajectory, *SteerTrack* further develops a *geometrical transformation*-based method for estimating the rotation angle of steering wheel in 3D driving environments by projecting the steering wheel to a 2D ellipse. Through extensive experiments in real driving environments with 5 volunteers for several weeks, *SteerTrack* can achieve an average error of 4.61 degree for estimating the rotation angle of steering wheel.

## I. INTRODUCTION

Recent decades have witnessed tremendous development in Advanced Driving Assistant Systems (ADAS) based on mobile devices [1]. Unlike the built-in ADAS leveraging advanced pre-implemented sensors (e.g., cameras, radars and LiDAR), mobile devices-based ADAS are cost-effective, portable and powerful enough to enhance vehicle systems, especially for providing safety services. There have been existing works on providing safety services based on mobile devices by sensing dynamics of vehicles [2] [3] including the vehicle speed, lane changes and other conditions. These works are limited in providing time-sensitive information as they can only capture the vehicles' conditions, which are delayed from drivers' operations. Other works put their efforts on exploring mobile devices to monitor the behaviors of drivers [4] [5]. These approaches can not quantitatively relate the behaviors of drivers to vehicle conditions.

Since the steering wheel is directly turning operations of a driver to vehicle conditions, tracking the usage of steering wheel provides fundamental techniques for monitoring the vehicle dynamics and identifying unsafe driving behaviors.

Particularly, the rotation angle of steering wheel is extremely useful in detecting lane changes, making turns, unsafe driving behaviors like under-steer or over-steer [6] and even fatigues [7]. So monitoring the rotation angle of steering wheel can provide real-time and fine-grained services for safety driving. Most recently, Karatas et al. [8] present a method to track the rotation angle of steering wheel based on smartwatches. However, this approach requires drivers to wear a smartwatch, which is not popular enough among drivers.

Moving along this direction, a device-free steering tracking approach is essential to achieve real-time and fine-grained safety services for drivers. Since movements of a steering wheel are directly related to a driver's operations, tracking the rotation angle of steering wheel can be grounded on tracking the movement trajectory of a driver's hands. We study whether it is possible to utilize acoustic signals to track the operations of driver's hands on the steering wheel, as acoustic signals have been proved feasible in sensing moving objects

without deploying customized hardware on mobile devices [9]–[12]. Our objective is to build a system for tracking the rotation angle of steering wheel leveraging audio devices on a smartphone. To realize the acoustic-based tracking, we face several challenges in practice. Firstly, in real driving environments, acoustic signals are more easily suffered from multi-path transmitting with signal fading and scattering. Secondly, a driver may have different steering maneuvers, i.e., steering with right hand only, with left hand only or with both hands, so movements of a driver's both hands need to be tracked at the same time. Thirdly, we should leverage the limited audio devices on off-the-shelf smartphones to track the rotating trajectory of steering wheel in 3D driving environments.

In this paper, we propose an acoustic-based device-free steering tracking system, *SteerTrack*, which can track the rotation angle of steering wheel in real time based on audio devices on smartphones. In *SteerTrack*, we first built an ultrasonic signal field inside of a vehicle by designing the transmitted acoustic signal as periodic signal blocks to identify the echoes from moving objects. Based on the acoustic signal field, the echoes reflected by a driver's hands can be identified through analyzing *relative correlation coefficient (RCC)* between the received signal and transmitted signal, and further the movement trajectory of a driver's both hands can be tracked at

the same time based on *reference frame*. Afterwards, by *geometrical transformations*, we find that the steering wheel appears to be an ellipse projection on a 2D plane through the central axis of smartphone and further derive the formula of the ellipse. Finally, given the formula of ellipse projection and the movement trajectory of driver's hands, *SteerTrack* can realize the rotation angle estimation of steering wheel through the geometrical relation of projection. Our extensive experiments validate the high-accuracy and feasibility for using our system in real driving environments.

We highlight our main contributions as follows:

- We design a steering tracking system, *SteerTrack*, which leverages audio devices on off-the-shelf smartphones to track the fine-grained rotation angle of steering wheel in real time for safety driving.
- We construct a data communication channel for acoustic signals to track moving objects with a smartphone and further track the movement trajectory of a driver's hands under different steering maneuvers.
- We apply geometrical transformations to map the steering wheel to a 2D ellipse to estimate the rotation angle of steering wheel in 3D driving environments.
- We conduct extensive experiments in real driving environments and the results show that *SteerTrack* achieves an average error of 4.61 degrees for tracking the rotation angle of steering wheel.

The rest of the paper is organized as follows. System design of *SteerTrack* is presented in Section II. Acoustic signal processing procedures are shown in Section III. We present hand movement tracking approaches in Section IV. The estimation for the rotation angle of steering wheel is presented in Section V. We evaluate the performance of *SteerTrack* and present the results in Section VI. We review related work in Section VII, and conclude our work in Section VIII.

## II. SYSTEM DESIGN

In this section, we first discuss the basic idea about acoustic-based steering tracking and the corresponding challenges, then we present the system overview.

### A. Basic Idea

When driving, movements of a steering wheel are directly related to a driver's operations. Therefore, the movement trajectory of the driver's hands can be exploited to track the rotation angle of steering wheel. Inspired by sonar system, we turn a smartphone to an active sonar in driving environments, which can be used to track the movement trajectory of a driver's hands.

Specifically, acoustic signals are transmitted by the speaker on a smartphone, then reflected by a driver's hands, and received by two microphones on the smartphone, respectively. As is shown in Fig.1. Assuming the steering wheel and the smartphone are in the same plane, we can utilize the time of arrival (ToA) [13] to obtain the position of the driver's hands leveraging the two microphones and one speaker in the smartphone. Given the coordinate system in Fig.1, the

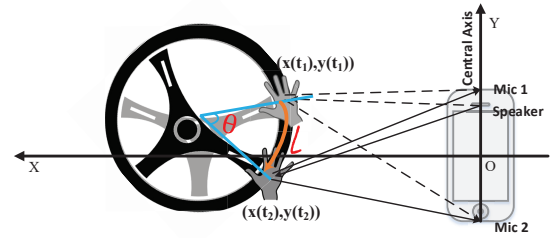


Fig. 1. Illustration of tracking the rotation angle of steering wheel with audio devices on a smartphone in a 2D plane.

coordinate of a hand at time  $t$  can be obtained as  $(x(t), y(t))$  by calculating the intersection point of two ellipse related to the two microphones and the speaker [11] [12] [14]. Assuming the driver rotates the steering wheel during a time period  $T$ , then through continuously tracking movements of driver's one hand in  $T$ , the rotation trajectory of steering wheel from  $t_1$  to  $t_2$  in  $T$  can be calculated as

$$l = \sum_{t=t_1}^{t_2-\Delta t} \sqrt{(x(t+\Delta t) - x(t))^2 + (y(t+\Delta t) - y(t))^2}, \quad (1)$$

where  $\Delta t$  is the sample period. Thus, the rotation angle of steering wheel  $\theta$  from  $t_1$  to  $t_2$  can be obtained as  $\theta = \frac{180 \times l}{\pi r}$ , where  $r$  is the radius of steering wheel.

### B. Challenges

In real driving environments, in order to track the rotation angle of steering wheel using audio devices on smartphones, a number of challenges need to be addressed.

- In the space of a driver's cab, after transmitted by the speaker in a smartphone, acoustic signals propagate to the microphones of the smartphone through multiple path, such as the car roof, seats, etc., with extra fading and scattering. To track the movement of a driver's hands, the system need to identify echoes reflected by the driver's hands from other objects in composite received signals.
- In real driving scenario, instead of always using both hands to operate the steering wheel, a driver often uses one hand to rotate the steering wheel, while uses the other hand to shift the gear or adjust the instrument panel, etc. So in order to accurately measure the rotation angle of steering wheel, the system need to track two moving objects (two hands) at the same time for obtaining rotation trajectory of steering wheel under different steering maneuvers. To the best of our knowledge, the problem of acoustic-based tracking for more than one moving object is remained open.
- Since audio devices on off-the-shelf smartphones are limited (commonly one speaker two microphones), a smartphone can only track the trajectory of a moving object in a 2D plane through the central axis of smartphone. However, in real driving environments, usually the steering wheel and the smartphone are in different planes. So the system need to estimate the rotation angle of steering wheel in 3D driving environment based on the projection of steering wheel in the 2D plane.

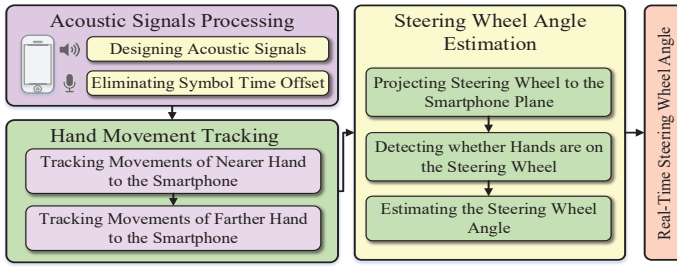


Fig. 2. System architecture of *SteerTrack*.

### C. System Overview

In order to realize the device-free steering tracking using a smartphone, we present a steering tracking system, *SteerTrack*, which estimates the rotation angle of steering wheel by analyzing the movement trajectory of a driver's both hands with acoustic signals. *SteerTrack* does not depend on any pre-deployed infrastructure and additional hardware. The architecture of *SteerTrack* is shown in Fig.2. The whole system is divided into three parts: *Acoustic Signals Processing*, *Hand Movement Tracking* and *Steering Wheel Angle Estimation*.

*SteerTrack* first builds an acoustic signal field as continually transmitting acoustic signals by the speaker and receiving echoes by microphones on a smartphone. In the transmitting end, *SteerTrack* sets the acoustic signal as a signal block transmitted periodically with separation in a communication channel. In the receiving end, *SteerTrack* uses the property of the transmitted signal to eliminate *symbol time offset* (STO).

After the acoustic signal field is constructed, a driver's hands can be tracked in *Hand Movement Tracking* section. For the hand nearer to the smartphone, *SteerTrack* uses *relative correlation coefficient* (RCC) to identify the echo reflected by the hand in the received signal. For the hand farther to the smartphone, its reflected echo is identified by applying *reference frame*. Combined these methods, *SteerTrack* can track movements of both hands for a driver on a 2D plane through the central axis of smartphone (i.e., smartphone plane).

Afterwards, *SteerTrack* estimates the rotation angle of steering wheel based on the movement trajectory of a driver's both hands. The steering wheel first is projected as an ellipse on the smartphone plane. Then, *SteerTrack* detects whether a driver's hands are on the steering wheel based on the tracked hands movement trajectory and the ellipse projection of steering wheel. Finally, the rotation angle of steering wheel is estimated.

## III. ACOUSTIC SIGNALS PROCESSING

For the steering tracking, we first need to build an acoustic signal field using audio devices on a smartphone. In this section, we present an acoustic signal processing method in both the transmitted end (a speaker) and the received end (two microphones). Fig.3 illustrates the structure of acoustic signal transmission of *SteerTrack* in both ends.

### A. Designing Acoustic Signals in the Transmitting End

For building an acoustic signal field, we first need to construct a data communication channel for acoustic signals

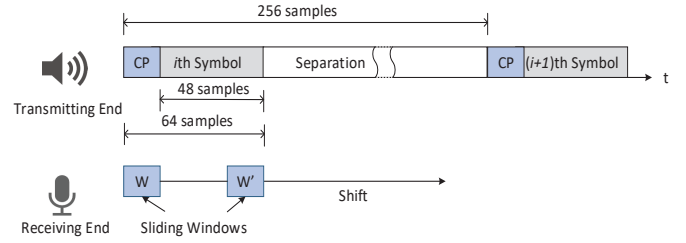


Fig. 3. Structure of the acoustic signal transmission in an acoustic signal field.

with a carrier. In practice, we choose the carrier as a sinusoidal of  $f = 20kHz$  to avoid been interfered by noises in driving scenario (i.e., wind, music, talking, etc.) and heard by people. With the carrier, a data sequence is transmitted. Particularly, to achieve high quality echoes, the length of the sequence is set to be 48 according to empirical study [15], i.e., these 48 samples form the transmitted signal symbol. We further extend the transmitted signal symbol by adding a cyclic prefix (CP) of 16 samples to its beginning, as shown in Fig.3. Then, the 64 samples form a signal block and is transmitted periodically by the speaker of a smartphone.

In order to capture echoes reflected by driver's hands, the signal block is transmitted periodically by the speaker with separations. The separation is to ensure that the echo of a signal block reflected by the hands can be received by the microphones before the speaker transmits next signal block [12]. Considering the real driving environments, the length of the separation is set to be 192 samples so that all echoes within the range of  $0.75m$  can be captured without being interfered by the next signal block, as shown in Fig.3.

### B. Eliminating Symbol Time Offset in the Receiving End

Since the signal block is transmitted periodically in the transmitting end, it is essential to determinate the start point of each signal block for the received signal in the receiving end. However, even embedded in the same smartphone, the speaker and microphones are not perfectly synchronized, resulting in a time offset in each period between the transmitted signal and received signal, i.e., *symbol time offset* (STO). To eliminate STO, we add a cyclic prefix (CP) in the beginning of each transmitted signal block, which is a replica of the last 16-samples data in the 48-samples signal symbol. CP and the corresponding data part thus can be used for STO elimination.

Specifically, we apply a pair of sliding windows,  $W$  and  $W'$ , to eliminate STO, as shown in Fig.3. The length of each window is  $L_0 = 16$  samples and the separation between two windows is 32 samples. According to the transmitted signal, the similarity between  $W$  and  $W'$  is maximized when the beginning of  $W$  is aligned to the beginning of CP in a transmitted signal block and  $W'$  is aligned to the end of the block. So STO can be estimated when the difference between these two sliding windows is minimized as:

$$\delta = \arg \min_k \left\{ \sum_{i=k}^{k+L_0} (|W_i| - |W'_i|)^2 \right\}, \quad (2)$$

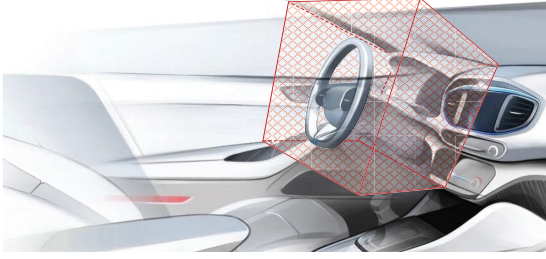


Fig. 4. The area that *SteerTrack* prefer driver to place the smartphone in the real driving scenario with and without a co-pilot.

where  $k$  is sliding over the received signal with step of 1 sample. Once the STO,  $\delta$ , is estimated, we can calibrate the start point of each signal block in the received signal. Finally, an acoustic signal field for steering tracking is built.

#### IV. HAND MOVEMENT TRACKING

According to the distance from the smartphone, we define the hand nearer to the smartphone as *Nearer Hand* and the hand farther to the smartphone as *Farther Hand* for a driver. Since a driver may have different steering maneuvers, i.e., steering with *Nearer Hand* only, with *Farther Hand* only or with both hands. So movements of a driver's *Nearer Hand* and *Farther Hand* need to be tracked at the same time.

Additionally, to realize the tracking, there is a basic assumption that the hands of a driver are the nearest *independent moving objects* with respect to the smartphone. It is obvious that the assumption is highly related to the smartphone's placement in a vehicle, where some places satisfies the assumption, while others are not. According to our empirical study involving multiple drivers and varies kinds of cars, we find that the assumption is valid with the smartphone placed in the red area shown in Fig.4. The area covers the front of a driver, which is most commonly used by drivers to place their smartphones. For example, usually drivers prefer to put their smartphones on the instrument panel for GPS, hands-free calls, etc. For active steering tracking, it is reasonable for drivers to put their phones in these places instead of places that are not satisfied the assumption (e.g., the pockets of the clothes). Moreover, We explore the impact of smartphone placements to the performance of *SteerTrack* in the Section VI-F.

##### A. Tracking Movements of Nearer Hand to the Smartphone

*SteerTrack* first tracks movements of *Nearer Hand* for a driver based on acoustic signals. After acoustic signals are transmitted from the speaker of a smartphone, some signals directly propagate to the microphones, and others are reflected by different obstructions they encounter, e.g., the car roof, the seats and so on, and then received by the microphones of the smartphone, which is referred as multi-path propagation.

To identify the echo reflected by *Nearer Hand* in the received acoustic signals with multi-path propagation, we explore the correlation between the received signal and transmit-

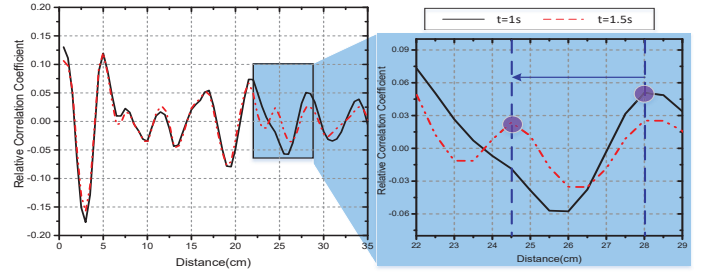


Fig. 5. RCC profiles of the received signal for a driver with a hand moving towards the smartphone at  $t=1s$  and  $t=1.5s$ .

ted signal block by computing relative correlation coefficient (RCC), which is defined by us as:

$$R(i, j) = \frac{Cov(i, j)}{\sqrt{Cov(i, i)Cov(j, j)}} \times \frac{\sum_{k=1}^L (|i_k|)/L}{\sum_{k=1}^L (|j_k|)/L}, \quad (3)$$

where  $i$  and  $j$  are vectors of length  $L$ ,  $Cov(i, j)$  represents the covariance of  $i$  and  $j$ ,  $Cov(i, i)$  and  $Cov(j, j)$  represents the variance of  $i$ ,  $j$ , respectively. Specifically, we construct a sliding window of 64 samples for the received signal and compute RCC between the signal in the sliding window and the transmitted signal block. Fig.5 shows RCC profiles for the received signal at  $t = 1s$  and  $t = 1.5s$  in a real driving environment, where a driver moves *Nearer Hand* towards the smartphone placed on the instrument panel. To better show the distance relationship between the smartphone and obstructions, we translate the received time into the distance between the object and the smartphone leveraging ToA of acoustic signals. In Fig.5, each peak of RCC profiles represents an echo from an obstruction. Concretely, the static peaks represent obstructions that not move during the  $0.5s$ , such as the seats, car roof, etc., while moving peaks are related to moving objects such as the driver's hands. As we can see from the sub-figure, when the drive's *Nearer Hand* moves from  $28cm$  at  $t = 1s$  to  $24.5cm$  at  $t = 1.5s$  with respect to the smartphone, there is a corresponding moving peak in RCC profiles.

Given the position of moving peaks, then movements of *Nearer Hand* with respect to the smartphone can be tracked. However, it can be seen from Fig.5 that there are several moving peaks occurs when the driver moves *Nearer Hand*. The reason is that when the hand moves, the elbow, arm and other body parts may move consequently at the same time, causing several other changes in the position of peaks in RCC profiles. Practically, *SteerTrack* chooses the first moving peak to represent movements of *Nearer Hand* because it is the nearest moving object to the smartphone when placing smartphone in valid places shown in Fig.4.

##### B. Tracking Movements of Farther Hand to the Smartphone

In addition to track movements of *Nearer Hand*, *SteerTrack* also needs to track movements of *Farther Hand* for a driver. As we mentioned in Section.IV-A, *SteerTrack* identifies the first moving peak in RCC profiles as the echo reflected by *Nearer Hand*. In our assumption, *Farther Hand* is the closest moving object to the smartphone except *Nearer Hand*. However, we

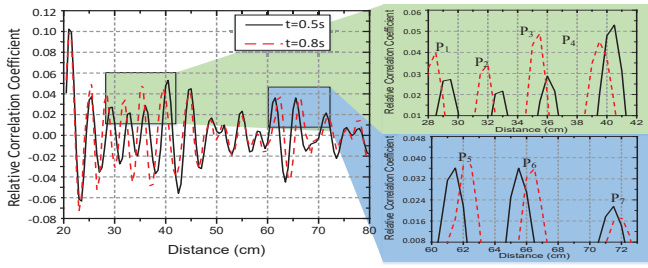


Fig. 6. RCC profiles of the received signal for a driver with Nearer Hand moving towards the smartphone and Farther Hand moving away from the smartphone at  $t=0.5s$  and  $t=0.8s$ .

can not simply identify the second moving peak in RCC profiles as the echo reflected by Farther Hand, as movements of Nearer Hand may bring movements of corresponding body parts, such as elbow, arm, etc.

To capture movements of Farther Hand, we need to eliminate all echoes reflected by Nearer Hand and corresponding body parts. Due to physical connections, the movement patterns of Nearer Hand and corresponding body parts are similar, so peaks related to these parts in RCC profiles also have similar movement patterns. Thus, *SteerTrack* utilizes the physical concept of *reference frame* to set the first moving peak as a reference peak, then peaks with the similar movement patterns as the reference peak can be considered as related to Nearer Hand and be removed. We describe the movement patterns of a peak in RCC profiles by Distance Difference Sequence (DDS), which is the distance difference for the peak between two neighboring RCC profiles over a sequence of RCC profiles.

Fig.6 shows RCC profiles for the received signal at  $t = 0.5s$  and  $t = 0.8s$  in a real driving environment, where Nearer Hand of a driver moves towards the smartphone and Farther Hand moves away from the smartphone. As shown in Fig.6, *SteerTrack* first scans RCC profiles to find all the moving peaks as  $\{P_1, P_2, \dots, P_7\}$ . Then, we calculate the correlation between DDS of the first moving peak and DDS of each moving peak using the equation  $Corr(i, j) = \frac{Cov(i, j)}{\sqrt{Cov(i, i)Cov(j, j)}}$ . If  $Corr(DDS_1, DDS_i)$  is greater than a threshold  $h$ , then peak  $i$  is considered as a moving peak reflected by Nearer Hand and corresponding body parts (i.e.,  $P_1, P_2, P_3, P_4$  in Fig.6). Otherwise, peak  $i$  is considered as a moving peak caused by a different moving object independent to Nearer Hand (i.e.  $P_5, P_6, P_7$  in Fig.6). Similar to tracking Nearer Hand, we choose the first moving peak not related to Nearer Hand (i.e.,  $P_5$ ) to represent movements of Farther Hand.

Note that in the 1-dimension case showed in Fig.6, it is possible that movement patterns of Nearer Hand and Farther Hand are too similar to be distinguished (e.g., both hands move towards or reverses the smartphone). However, the movement patterns of two hands are unlikely to be similar in the 2-D plane captured by a speaker and two microphones on a smartphone. Thus *SteerTrack* is able to get the movement trajectory of a driver's both hands.

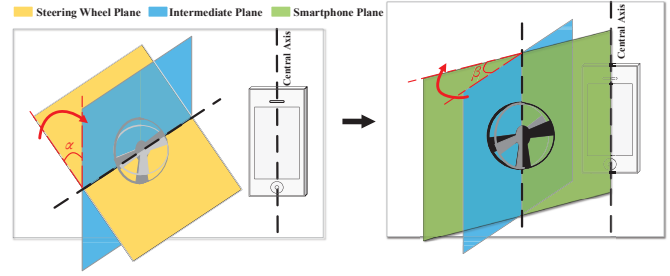


Fig. 7. Projection procedure of steering wheel from the steering wheel plane to the smartphone plane.

## V. STEERING WHEEL ANGLE ESTIMATION

With limited audio devices (a speaker and two microphones) on a smartphone, the movement trajectory of a driver's both hands can only be measured in a 2D plane through the central axis of smartphone, which is denoted as the *smartphone plane*. To estimate the rotation angle of steering wheel, *SteerTrack* first projects the steering wheel inside of a vehicle to the smartphone plane, and then determine whether the hands of a driver are on the steering wheel. Afterwards, the rotation angle of steering wheel can be estimated based on the movement trajectory of the hands when they are on the steering wheel.

### A. Projecting the Steering Wheel to the Smartphone Plane

In real driving environments, the steering wheel tracked by a smartphone is a projection of the real steering wheel in the smartphone plane. Fig.7 shows the projection procedures of the steering wheel from the steering wheel plane to the smartphone plane, which contains two geometrical transformations.

Specifically, we model a steering wheel as a geometrical circle. Assuming the origin is at the center of steering wheel and the  $x$  axis is the horizontal line crossing the origin, the circle can be denoted as  $x^2 + y^2 = r^2$  in the steering wheel plane. Then, we rotate the steering wheel plane along the  $x$  axis, until the plane is parallel to the central axis of smartphone, the new plane is denoted as the intermediate plane, as shown in the left figure of Fig.7. Keep the origin and  $x$  axis unchanged and given the rotating angle of the plane as  $\alpha$ , then the formula of steering wheel projection in the intermediate plane can be denoted as

$$\frac{x^2}{r^2} + \frac{y^2}{r^2 \cos^2 \alpha} = 1. \quad (4)$$

Afterwards, we rotate the intermediate plane along the diameter of steering wheel that is parallel to the central axis of smartphone until the plane goes through the smartphone's central axis, as shown in the right figure of Fig.7. Similar to the first transformation, given the rotating angle of the plane as  $\beta$ , then the formula of steering wheel projection in the smartphone plane can be denoted as

$$\frac{x^2}{r^2 \cos^2 \beta} + \frac{y^2}{r^2 \cos^2 \alpha} = 1. \quad (5)$$

According to Eq.5, the projection of steering wheel in the smartphone plane is a deterministic ellipse once the position of smartphone is fixed.

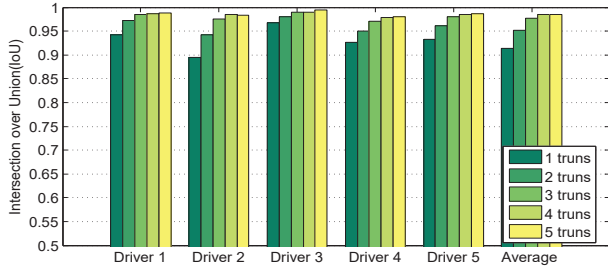


Fig. 8. IoU of the constructed ellipse and baseline ellipse under different numbers of turns.

### B. Detecting whether Hands are on the Steering Wheel

Although the formula of steering wheel projection is already deduced as Eq.5, there are unknown parameters, i.e.,  $\alpha$  and  $\beta$ , which can not be measured in real driving environments. So, to track the rotation trajectory of steering wheel, we propose a fitting-based approach to calculate the formula of steering wheel's projection in the smartphone plane.

Since *SteerTrack* tracks objects in a 2D plane through the central axis of smartphone, we set the origin at the central point of smartphone. Because the formula of steering wheel projection is an ellipse in the smartphone plane, the formula can be denoted as

$$Ax^2 + Bxy + Cy^2 + Dx + Ey + 1 = 0, (B^2 - 4AC < 0). \quad (6)$$

In Eq.6, there are 5 parameters, i.e.,  $A, B, C, D, E$ . Theoretically, any 5 different points on the ellipse can be used to determine the parameters. In practice, if more points are sampled and the points are distributed more evenly on the ellipse, the parameter estimation will be more accurate. Since the movement trajectory of a driver's hands is on the ellipse when the driver rotates the steering wheel, we can track the positions of the driver's hands to compute the parameters.

Specifically, when a driver makes turns, *SteerTrack* tracks the movement trajectory of the driver's hands to sample points, i.e., positions of the driver's hands. At the beginning of a trip, a driver usually operates the steering wheel for making multiple turns to pull out of a parking lot or drive on local streets before getting onto main roads [16]. For each turn, *SteerTrack* randomly samples  $N$  ( $N \geq 5$ ) points on the movement trajectory of the driver's hands. After making  $k$  turns, with  $N \times k$  points, the parameters of the ellipse formula,  $A, B, C, D, E$ , are estimated solving the overdetermined linear equations,  $Ax_i^2 + Bx_i y_i + Cy_i^2 + Dx_i + Ey_i + 1 = 0, (i = 1, 2, \dots, N \times k)$ , with least square fitting.

We demonstrate the feasibility of our method by asking five divers to drive their cars with a smartphone constructing the projection formula of steering wheel in the smartphone plane through making turns. After each turn, 5 points are sampled randomly. Additionally, we construct a baseline ellipse by rotating the steering wheel to a full circle in 10s, meanwhile 10 points of the hand position are sampled every second, and then parameters of the baseline ellipse are computed with our fitting method. Fig.8 shows the performance of our method by comparing the constructed ellipse after making  $k$  turns

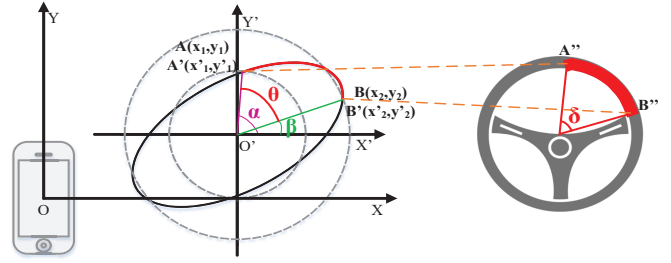


Fig. 9. Illustration of estimating the rotation angle of steering wheel.

to the baseline ellipse. We use the intersection over union (IoU) to evaluate the similarity of these two ellipses, which is calculated as

$$IoU = \frac{Constructed\ Ellipse \cap Baseline\ Ellipse}{Constructed\ Ellipse \cup Baseline\ Ellipse}. \quad (7)$$

As shown in Fig.8, after only 3 turns, *IoU* for every driver is greater than 0.97, showing that the constructed ellipse is very closed to the baseline ellipse. The result confirms the feasibility of constructing ellipse trajectory with our methods.

Based on the constructed ellipse, *SteerTrack* now can obtain the rotation trajectory of steering wheel with different steering maneuvers. If Nearer Hand of the driver is on the ellipse, *SteerTrack* takes the movement trajectory of Nearer Hand as the rotation trajectory of steering wheel. Otherwise, *SteerTrack* takes the movement trajectory of Farther Hand as the rotation trajectory of steering wheel. For the special case that none of the hands are on the steering wheel, *SteerTrack* ignores the movement trajectory of both hands.

### C. Estimating the Steering Wheel Angle

*SteerTrack* tracks the rotation angle of steering wheel based on the rotation trajectory of steering wheel in the smartphone plane. In fact, during the procedure that maps the steering wheel to ellipse projection in the smartphone plane, only linear transformation, such as rotating and scaling, are performed. Thus, the rotation angle of ellipse in the smartphone plane is equal to the rotation angle of real steering wheel, i.e.,  $\angle\theta = \angle\delta$ , as shown in Fig.9.

As shown in Fig.9, the movement trajectory of a driver's hand on the ellipse from  $A(x_1, y_1)$  to  $B(x_2, y_2)$  is measured. To estimate  $\angle\theta$ , we first change the coordinate system from  $XoY$  to  $X'o'Y'$  by moving the origin from the smartphone to the center of ellipse, which has the coordinate

$$(X_c, Y_c) = \left( \frac{BE - 2CD}{4AC - B^2}, \frac{BD - 2AE}{4AC - B^2} \right) \quad (8)$$

under the ellipse described by Eq.6. Then, in the new coordinate system,  $A$  and  $B$  has the coordinate  $A(x'_1, y'_1)$  and  $B(x'_2, y'_2)$ , respectively. As shown in Fig.9, the center angle for  $A$  and  $B$  with respect to the  $x$  axis can be calculated as  $\angle\alpha$  and  $\angle\beta$ . Then,  $\angle\theta$  can be estimated as  $\angle\theta = \angle\alpha - \angle\beta$ . So the rotation angle of steering wheel can be estimated as  $\angle\delta = \angle\theta$ . By continuously computing  $\angle\delta$ , *SteerTrack* can finally tracks the rotation angle of steering wheel with acoustic signals.



Fig. 10. Telematics BOX records the ground truth for the rotation angle of steering wheel.

## VI. EVALUATION

In this section, we evaluate the performance of *SteerTrack* from real driving environments with 5 volunteers for 6 weeks.

### A. Experiments Setup and Methodology

We implement *SteerTrack* as an Android App and install it on 5 different types of smartphones, which are Google Pixel, HTC U Ultra, Samsung Galaxy S6, LG G4 and Huangwei Mate8, respectively. *SteerTrack* is run by 5 drivers with distinct vehicles. During the driving, the smartphone are placed in three common places, i.e., the instrument panel, cab door and cupholder, and drivers are free to playing music, adjust the seat, open the window, etc., when driving.

Meanwhile, the ground truth for the rotation angle of steering wheel is obtained from *Telematics BOX*, which is installed in each vehicle, as shown in Fig.10. Additionally, each vehicle is implemented with a camera for recording drivers' hand movements while driving. We conduct our experiments for 6 weeks, from 5th May 2017 to 25th June 2017, during which all the daily driving, such as commuting to work, shopping, etc., is recorded.

To evaluate the performance of *SteerTrack*, when drivers make turns, we compare the estimated rotation angle of steering wheel ( $\theta_{estimated}$ ) to the ground truth ( $\theta_{real}$ ). The most important metric in our experiments is *absolute error*, which is defined as  $\delta_{\theta} = |\theta_{real} - \theta_{estimated}|$ . After data collection, 4118 turns of different steering wheel rotation ranges are collected from the 5 drivers, as shown in Table.I.

### B. Overall Performance

Fig.11 shows the cumulative distribution function (CDF) of  $\delta_{\theta}$  for turns with different steering wheel rotation ranges. From the figure, we can see that  $\delta_{\theta}$  increases as the steering wheel rotation range becomes larger. Concretely, 80%  $\delta_{\theta}$  are lower than 2.31 degree, 3.39 degree, 4.73 degree and 5.66 degree for  $[0^{\circ}, 30^{\circ})$ ,  $[30^{\circ}, 60^{\circ})$ ,  $[60^{\circ}, 90^{\circ})$  and  $\geq 90^{\circ}$ , respectively. For

TABLE I  
TURNS OF DIFFERENT STEERING WHEEL ROTATION RANGES COLLECTED FROM FIVE VEHICLES

Vehicle ID	1	2	3	4	5
$[0^{\circ}, 30^{\circ})$	21	15	28	17	33
$[30^{\circ}, 60^{\circ})$	154	93	107	161	147
$[60^{\circ}, 90^{\circ})$	507	465	491	679	588
$\geq 90^{\circ}$	279	253	342	322	299
Total	961	826	968	1179	1067

all turns, 50%  $\delta_{\theta}$  are lower than 1.72 degree and 80%  $\delta_{\theta}$  are lower than 4.02 degree.

We compare *SteerTrack* with the smartwatch-based approach [8] and steering-wheel-mounted sensor [17]. For [8], we implement the smartwatch-based approach leveraging 5 MOTO 360 smartwatches for 5 drivers. For [17], we implement a steering-wheel-mounted sensor in each vehicle. Fig.12 shows the average  $\delta_{\theta}$  of *SteerTrack* and these two approaches under different steering wheel rotation ranges. From the figure, we observe that the average  $\delta_{\theta}$  increases as the steering wheel rotation range becomes larger for all three approaches. Moreover,  $\delta_{\theta}$  for steering-wheel-mounted sensor is very small as it directly measures the rotation angle of steering wheel. For *SteerTrack* and the smartwatch-based approach in [8], the smartwatch-based approach performs slightly better than *SteerTrack* when the steering wheel rotation range is small(i.e., in  $[0^{\circ}, 60^{\circ})$ ). When the rotation range becomes larger ( $\geq 60^{\circ}$ ), *SteerTrack* outperforms the smart watch-based approach. This is because when making turns with a small rotation range, drivers may finish the operation with hands on the steering wheel for the whole time, where the smartwatch-based approach can measure the  $\theta_{estimated}$  more accurate. However, in the case that rotation ranges are large, drivers prefer to change their hands to finish the operation. Then the smartwatch-based approach may miss the operation when driver uses the watch-less hand to operate the steering wheel. Since we can see from Table.I that the steering wheel rotation ranges are larger than  $60^{\circ}$  for most turns, *SteerTrack* can be more accurate than the smartwatch-based approach in most cases. While in the case of lane-change detection, the smartwatch-based approach may perform slightly better. Under our experiments, the overall average  $\delta_{\theta}$  for *SteerTrack* and smartwatch-based approach are 4.61 degree and 5.25 degree, respectively.

We also evaluate the average  $\delta_{\theta}$  for each of the 5 drivers and show the result as box plot in Fig.13. It can be observed from Fig.13 that although the distribution of  $\delta_{\theta}$  are different over drivers due to different driving habits, the highest  $\delta_{\theta}$  is no more than 9 degree, and the overall median of  $\delta_{\theta}$  is as low as 4.79 for the 5 drivers. It shows that *SteerTrack* could achieve fine-grained estimation for different drivers.

### C. Performance of Detecting Different Steering Maneuvers

According to the steering wheel estimation method presented in Section.V, *SteerTrack* can recognize three different steering maneuvers, i.e., steering with Near hand only, with Farther Hand only and with both hands. We let *SteerTrack* output a monitoring result (Nearer Hand case, Farther Hand case or both hands case) every 5s and compare each result to the ground truth in video. For all three steering maneuvers, the accuracy of the recognition is 97.73%. Moreover, the precision, recall and F-score (i.e.,  $\frac{2 \times \text{precision} \times \text{recall}}{\text{precision} + \text{recall}}$ ) for the comparison is showed in Fig.14. It can be seen from the figure that these three metrics are high for each case. Specifically, the precision is no less than 96.1%, while the recall is above 95.7%, and the F-score is more than 96.8%. Moreover, the recall for both hands case is nearly 100%, showing that

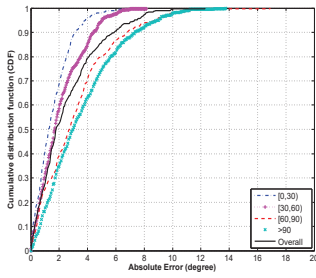


Fig. 11. CDF of  $\delta_\theta$  for turns under different steering wheel rotation ranges.

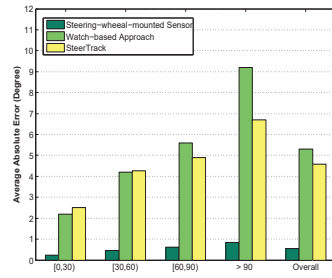


Fig. 12. Average  $\delta_\theta$  of *SteerTrack*, smartwatch-based [8] and sensor-based [17] approach.

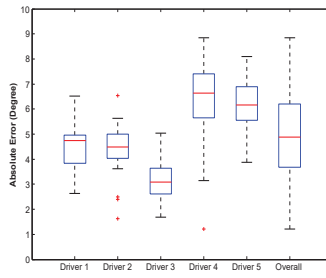


Fig. 13. Box plot of  $\delta_\theta$  for 5 drivers and the overall  $\delta_\theta$ .

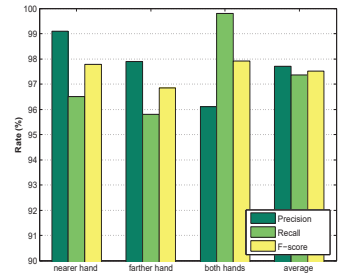


Fig. 14. Precision, Recall and F-Score for detecting three kinds of steering maneuvers.

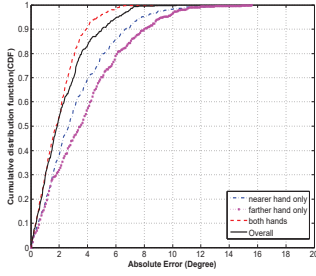


Fig. 15. CDF of  $\delta_\theta$  for three kinds of steering maneuvers.

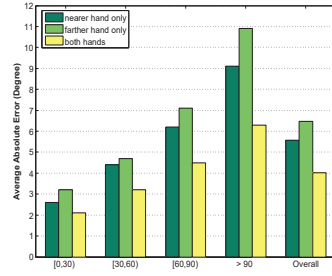


Fig. 16. Average  $\delta_\theta$  for three kinds of steering maneuvers.

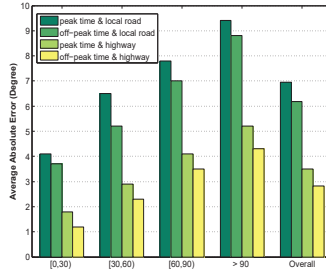


Fig. 17. Average  $\delta_\theta$  for different traffic conditions and road types.

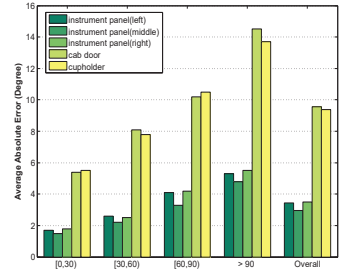


Fig. 18. Average  $\delta_\theta$  for different smartphone placement.

whenever a driver use both hands to drive, which is the most common case, *SteerTrack* can almost monitor it correctly.

#### D. Impact of Different Steering Maneuvers

We further study the impact of different steering maneuvers on the performance of *SteerTrack*. Fig.15 shows the cumulative distribution function (CDF) of  $\delta_\theta$  for three different steering maneuvers. From the figure we can see that  $\delta_\theta$  for using both hands is lowest, with 80%  $\delta_\theta$  lower than 3 degree, and  $\delta_\theta$  for using Farther Hand only is the highest among all three cases. The reason is that with only one hand operating the steering wheel, movements of the other hand become an interference to *SteerTrack*. Fig.16 shows the average  $\delta_\theta$  for different steering maneuvers under different steering wheel rotation ranges. It can be seen from the figure that the average  $\delta_\theta$  increase as the steering wheel rotation range becomes larger for all cases. Moreover, for larger steering wheel rotation range ( $\geq 60^\circ$ ), the average  $\delta_\theta$  for using both hands is lower than using one hand, which is useful as drivers usually use their both hands to steer when the rotation angle of steering wheel is large.

#### E. Impact of Traffic Conditions and Road Types

Traffic conditions and road types may influent drivers' driving behaviors and vehicle conditions, thus may have impacts on the performance of *SteerTrack*. We analyze the collected traces of different traffic conditions (during peak time and off-peak time) and different road types (on local road and highway), respectively. Fig.17 shows the average  $\delta_\theta$  for different steering wheel rotation ranges under all four combinations of road types and traffic conditions. From Fig.17, it can be seen that the average  $\delta_\theta$  is always lower than 10 degree at any combination of road types and traffic conditions. Moreover, during peak time, the average  $\delta_\theta$  is slightly larger than the average  $\delta_\theta$  during off-peak time because drivers

may perform complex operations with hands during heavy traffic, such as shifting gears or honking the horn, which may bring interferences to *SteerTrack*. For different road types, the average  $\delta_\theta$  on local roads is larger than the average  $\delta_\theta$  on highways. Because on local roads, vehicles may suffers from poor road conditions, such as bumpy roads, which is harmful for accurately estimating the rotation angle of steering wheel.

#### F. Impact of Smartphone Placement

In our experiments, we study the impact of smartphone placement for *SteerTrack* by placing smartphones on five different places in the vehicles, i.e., instrument panel (left side), instrument panel (middle part), instrument panel (right side), panel near cab door and cup-holder. Fig.18 shows the average  $\delta_\theta$  under  $\delta_\theta$  different steering wheel rotation ranges at all 5 placements. We can observe that *SteerTrack* achieves much lower average  $\delta_\theta$  when putting the smartphone on the instrument panel than the panel near cab door or cup-holder. The reason is that *SteerTrack* assumes that a diver's both hands are the nearest moving objects with respect to the smartphone. When the smartphone is put on the panel near cab door or cup-holder, movements of driver's legs or other body parts may bring extra errors to *SteerTrack*. To achieve better performance for *SteerTrack* to achieve active steering tracking, it is better for drivers to place smartphones in valid places shown in Fig.4, such as the instrument panel, position for placing GPS, etc.

## VII. RELATED WORK

There have been active research works in developing advanced driver-assistance systems (ADAS) in vehicles based on mobile devices [2]–[4], [8], [16], [18], [19]. Several works focus on detecting dynamics of vehicles to provide safety guidances for drivers [2] [3] [19]. Among these works, [3] monitors the speed of a vehicle based on the accelerator of a

smartphone, achieving better accuracy than GPS. [19] utilize smartphones to realize the lane-level tracking for vehicles on highways. [2] develops a system to detect several vehicle maneuvers. However, these approaches have not related the dynamics of vehicles to operations of drivers.

Other works using ADAS to enhance driving safety put their efforts on monitoring drivers' behaviors. [16] [18] detect whether a driver is using a mobile device when driving to prevent potential risk caused by distraction, which can not detect dangerous driving behaviors other than the phone use. [5] [20] leverage smartphones to recognize abnormal driving behaviors, but instead of quantitative analysis, only qualitative results can be provided. [4] leverages dual cameras of smartphones to detect road conditions and drivers status at the same time, but vision-based approaches provides unstable results depends on weather condition and smartphones placement. Although *SteerTrack* still has limitation in the smartphone placement, but the limitation is much less restricted compared to vision-based approaches.

For steering wheel-based ADAS, [6] presents a model to predict lane changes based on the rotation angle of steering wheel. However, [6] does not present a method to estimate the rotation angle of steering wheel. [17] estimates the rotation angles of steering wheel utilizing steering-wheel-mounted sensors. But this approach requires additional sensors, bringing extra cost and inconvenience for implementation. Recently, [8] presents a method to track the rotation angle of steering wheel based on smartwatches. However, this approach requires a smartwatch for a driver, which is not popular enough. Moreover, [8] can not track the rotation angle of steering wheel when drivers steer only with the watch-less hand.

In recent years, technologies are developed rapidly with acoustic signals to track moving objects. ApneaApp [21] uses FMCW to track heartbeats by analyzing periodic patterns of acoustic signals. AAmouse [22] realizes a virtual mouse leveraging audio devices of smartphones. CAT [10], LLAP [11], FingerIO [12] and Strata [14] tracks movements of a finger or a hand using a smartphone to transmitting and receiving acoustic signals, all these methods can achieve sub-centimeter tracking error. Unlike these works, which can only track the nearest moving object in a 2D plane, *SteerTrack* can estimate the rotation angle of steering wheel by tracking movements of both hands for a driver in 3D driving environments.

### VIII. CONCLUSION

In this paper, we address the problem of tracking the rotation angle of steering wheel in real time to improve driving safety. In particular, we propose a steering tracking system, *SteerTrack*, to estimate the rotation angle of steering wheel leveraging build-in audio devices on smartphones. *SteerTrack* builds an acoustic signal field inside of the vehicle and analyzes the echoes reflected from the driver's hands with *relative correlation coefficient (RCC)* and *reference frame* to track the movement trajectory of hands. Given the tracked movement trajectory, *SteerTrack* further develops a geometrical transformation-based method to estimate the rotation angle

of steering wheel in 3D driving environments by projecting the steering wheel to a 2D ellipse. The extensive experiments from real driving environments show that *SteerTrack* achieves low error for estimation the rotation angle of steering wheel. In the future, our work is focused on further releasing the limitation of the smartphone's placement for *SteerTrack*.

### ACKNOWLEDGMENT

This research is sponsored by National Natural Science Foundation of China (No. 61772338, 61420106010, 61772341, 61472254). This work is also supported by the Program for Changjiang Young Scholars in University of China, the Program for Shanghai Top Young Talents, and the National Top Young Talents Support Program.

### REFERENCES

- [1] T. News, "Us: Mobileye intros smartphone connected driver assistance (adas) technology." [Online]. Available: <http://telematicsnews.info/2012/01/12/>, 2012.
- [2] D. Chen, K.-T. Cho, et al., "Invisible sensing of vehicle steering with smartphones," in *Proc. Mobisys'15*, pp. 1–13, ACM, 2015.
- [3] H. Han, J. Yu, H. Zhu, Y. Chen, J. Yang, Y. Zhu, G. Xue, and M. Li, "Senspeed: Sensing driving conditions to estimate vehicle speed in urban environments," in *Proc. INFOCOM'14*, pp. 727–735, IEEE, 2014.
- [4] C.-W. You, N. D. Lane, et al., "Carsafe app: Alerting drowsy and distracted drivers using dual cameras on smartphones," in *Proc. Mobisys'13*, pp. 13–26, ACM, 2013.
- [5] X. Xu, H. Gao, J. Yu, Y. Chen, Y. Zhu, G. Xue, and M. Li, "Er: Early recognition of inattentive driving leveraging audio devices on smartphones," in *Proc. INFOCOM'17*, pp. 1–9, 2017.
- [6] K. Schmidt, M. Beggato, K. H. Hoffmann, and J. F. Krems, "A mathematical model for predicting lane changes using the steering wheel angle," *Journal of Safety Research*, vol. 49, no. 203, pp. 85–90, 2014.
- [7] Z. Li, S. E. Li, R. Li, B. Cheng, and J. Shi, "Online detection of driver fatigue using steering wheel angles for real driving conditions," *Sensors*, vol. 17, no. 3, p. 495, 2017.
- [8] C. Karatas, L. Liu, H. Li, et al., "Leveraging wearables for steering and driver tracking," in *Proc. INFOCOM'16*, 2016.
- [9] S. Gupta, D. Morris, S. Patel, and D. Tan, "Soundwave: using the doppler effect to sense gestures," in *Proc. CHI'12*, pp. 1911–1914, ACM, 2012.
- [10] W. Mao, J. He, and L. Qiu, "Cat: high-precision acoustic motion tracking," in *Proc. MOBICOM'16*, pp. 69–81, ACM, 2016.
- [11] W. Wang, A. X. Liu, and K. Sun, "Device-free gesture tracking using acoustic signals," in *Proc. MOBICOM'16*, pp. 82–94, ACM, 2016.
- [12] R. Nandakumar, V. Iyer, et al., "Fingerio: Using active sonar for fine-grained finger tracking," in *Proc. CHI'16*, pp. 1515–1525, ACM, 2016.
- [13] A. Malik, *RTLS for Dummies*. John Wiley & Sons, 2009.
- [14] S. Yun, Y.-C. Chen, et al., "Strata: Fine-grained acoustic-based device-free tracking," in *Proc. Mobisys'17*, pp. 15–28, ACM, 2017.
- [15] Y. S. Cho, J. Kim, W. Y. Yang, and C. G. Kang, *MIMO-OFDM wireless communications with MATLAB*. John Wiley & Sons, 2010.
- [16] Y. Wang, J. Yang, H. Liu, Y. Chen, M. Gruteser, and R. P. Martin, "Sensing vehicle dynamics for determining driver phone use," in *Proc. Mobisys'13*, pp. 41–54, ACM, 2013.
- [17] S. Lawoyin, X. Liu, D. Y. Fei, and O. Bai, "Detection methods for a low-cost accelerometer-based approach for driver drowsiness detection," in *Proc. SMC'14*, pp. 1636–1641, 2014.
- [18] J. Yang, S. Sidhom, et al., "Detecting driver phone use leveraging car speakers," in *Proc. MOBICOM'11*, pp. 97–108, ACM, 2011.
- [19] Z. Wu, J. Li, J. Yu, Y. Zhu, G. Xue, and M. Li, "L3: sensing driving conditions for vehicle lane-level localization on highways," in *Proc. INFOCOM'16*, pp. 1–9, IEEE, 2016.
- [20] Z. Chen, J. Yu, Y. Zhu, Y. Chen, and M. Li, "D3: Abnormal driving behaviors detection and identification using smartphone sensors," in *Proc. SECON'15*, pp. 524–532, IEEE, 2015.
- [21] R. Nandakumar, S. Gollakota, and N. Watson, "Contactless sleep apnea detection on smartphones," in *Proc. Mobisys'15*, pp. 45–57, ACM, 2015.
- [22] S. Yun, Y.-C. Chen, and L. Qiu, "Turning a mobile device into a mouse in the air," in *Proc. Mobisys'15*, pp. 15–29, ACM, 2015.